Bi-national conference on Detectors R&D - LPNHE Paris, November 18-20, 2025

Photo-Detector requirements for high-performance neutron identification in fragmentation events.

Iram B. Rivas Ortiz[a], Emanuele Maria Data[b], Veronica Ferrero[ab], Elisa Fiorina[a], Simona Giordanengo[ab], Felix Mas Milian[ac], Alessio Mereghetti[d], Diango Manuel Montalvan Olivares[ab], Francesco Pennazio[a], Marco Pullia[d], Sahar Ranjbar[b], Roberto Sacchi[ab], Anna Vignati[ab], Piergiorgio Cerello[a]

[a]Istituto Nazionale di Fisica Nucleare - INFN Torino, Italy; [b]University of Turin - Unito, Italy; [c]State University of Santa Cruz - UESC, Bahia, Brazil; [d]Centro Nazionale di Adroterapia Oncologica - CNAO, Pavia, Italy

Introduction

In **Particle Therapy**, interactions of protons and light ions with tissue produce **secondary neutrons** that contribute to the **out-of-field dose** in the patient [1]. In **Space Radiation**, Galactic Cosmic Rays interacting with spacecraft materials generate neutrons that can comprise a significant fraction of **astronaut exposure** [2]. In both contexts, **secondary neutrons with energies from 200 keV up to 500 MeV dominate the spectra** highlighting the need for reliable and optimized fast neutron detection systems.

The **Prompt Gamma Timing (PGT) system**, developed within the **INFN SIG_PNR project** was recently shown to be **sensitive to fast neutrons**. Originally designed for range verification in particle therapy, it measures the Time-Of-Flight (TOF) of each primary particle and the prompt gammas produced from nuclear interactions in the target through the combination of a beam sensor and a secondary detector [3].

Building upon this concept, the present study introduces a **method to measure neutron production from fragmentation events** using a **dedicated TOF multi-detector** setup featuring advanced **photo-detector technology** and **high-fluence rate** operation. Preliminary **measurements at CNAO (Pavia, Italy)** with a 398.84 MeV/u carbon ion beam irradiating a 5 mm graphite target (Fig. 1) demonstrate the **feasibility of fast neutron detection** and emphasize the need for **high-precision timing** from the photo detectors.

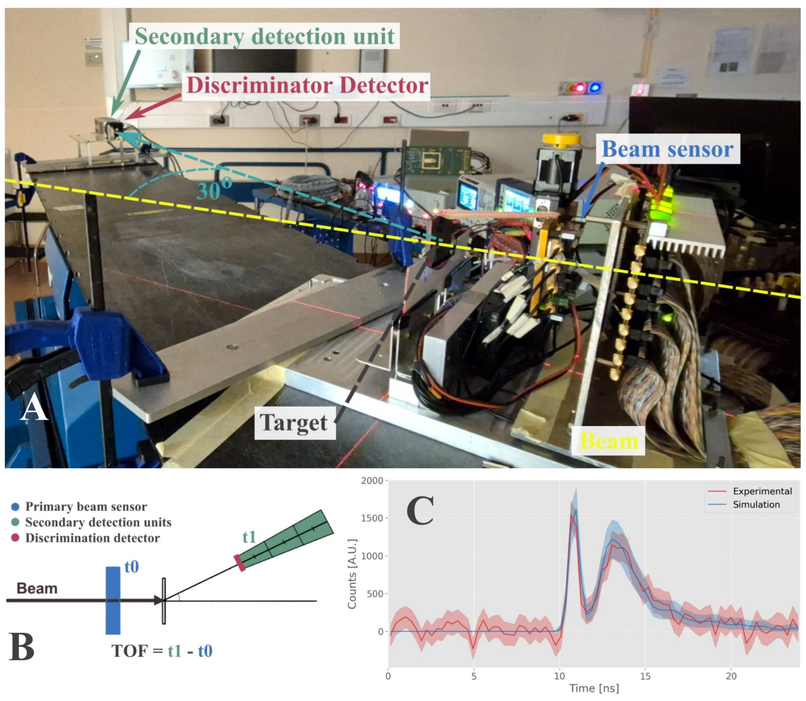

Figure 1 - (A) Experimental beam test at CNAO with 398.84 MeV/u carbon ions and 5 mm-thick graphite target. (B) Sketch of TOF measurement principle. (C) Monte Carlo (blue) and experimental TOF distributions (red). The shaded regions represent the 95% Confidence Intervals (CIs) per time bin.

Materials and Methods

The **proposed setup** (Fig. 2) includes a **primary beam sensor** for monitoring the incident beam, an **array of detection units** to record secondary particle signals, and a **discriminator detector** to reject charged particles. The array is positioned positioned **100 cm from the target** and at 30^0 polar angle relative to the beam axis to optimize **separation in time between gamma-ray** (first peak, Fig. 1C) **and neutron** (second peak, Fig. 1C) signals. **Monte Carlo (MC)** simulations were performed in FLUKA 2024.1 code, and TOF data is smeared to reproduce the required **150 ps resolution** for the analysis.

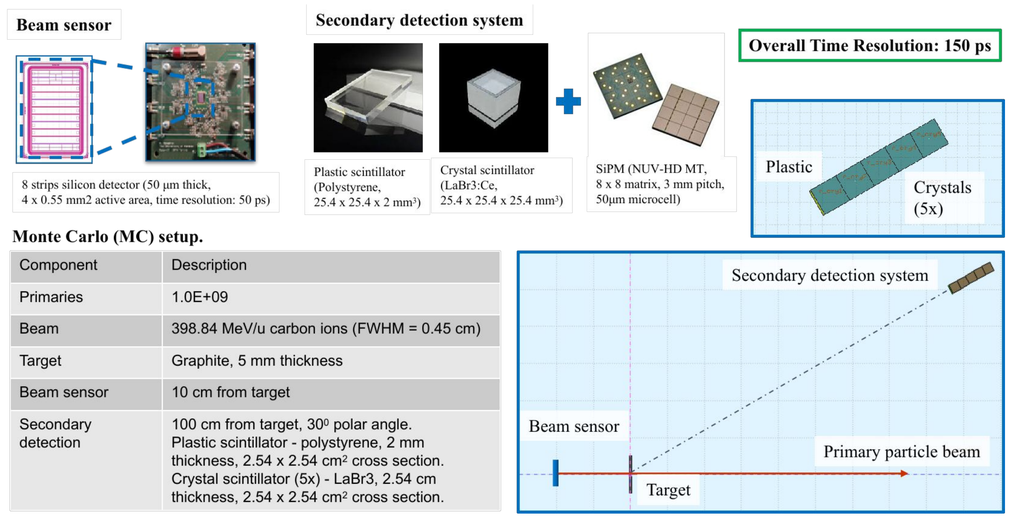

Figure 2 - Geometrical configuration and component selection for the proposed TOF multi-detector system for neutron measurements. Monte Carlo specifications used in the analysis.

Results and Discussion

MC simulations were conducted to assess the reliability of the TOF multi-detector system for neutron production due to fragmentation events. A **98.9% efficiency** was achieved for **charged-particle discrimination** using 2 mm-thick polystyrene. Among neutral particles passing through the veto detector, 59.4% are detected (**90.5% of gammas** and **57.3% of neutrons** records **energy deposition events** inside the secondary detection units).

Gamma peaks are used for **time resolution** verification, **transmission delay** estimation, and synchronization of the secondary detection units. Table 1 summarizes the number of detected gammas and neutrons (in bold) per second considering a beam rate of 1E+09 pps for each secondary detection unit. The system demonstrated reliable **gamma and neutron identification** based on TOF data, with **relative deviations of 2.2% and 2.4%** from MC truth, respectively.

Table 1 - MC truth and estimated gamma-rays and neutrons computed from TOF data at each secondary detection unit. Value expressed as particle per seconds (pps).

	Unit 1 [pps]	Unit 2 [pps]	Unit 3 [pps]	Unit 4 [pps]	Unit 5 [pps]
MC Truth	712 gammas **4793 neutrons**	386 gammas **3715 neutrons**	182 gammas **2937 neutrons**	102 gammas **2313 neutrons**	64 gammas **1624 neutrons**
Estimation	708 gammas **4642 neutrons**	374 gammas **3622 neutrons**	180 gammas **2856 neutrons**	107 gammas **2271 neutrons**	65 gammas **1588 neutrons**

Neutron kinetic energy distributions can be computed from TOF data using relativistic kinematics for each secondary detection units (Fig. 3). To estimate the **incoming neutrons** passing through the upfront surface of the detection system, a **Beer-Lambert curve fitting approach** is used. The model correlates the neutron counts at each unit to their relative depth within the secondary detection system. Using the detected neutrons per energy bin and corresponding depths, the incoming neutrons are estimated as a function of kinetic energy.

Beer-Lambert fitting approach:

$$N_i(E,\Omega)d = I_0(E,\Omega)[e^{\Sigma(E)d} - 1]e^{-\Sigma(E)di}$$

N_i [cm^{-3} s^{-1}]: Neutrons at crystal relative depth di.

Σ [cm^{-1}]: Total cross section.

I_0 [cm^{-2} s^{-1}]: Incoming neutrons.

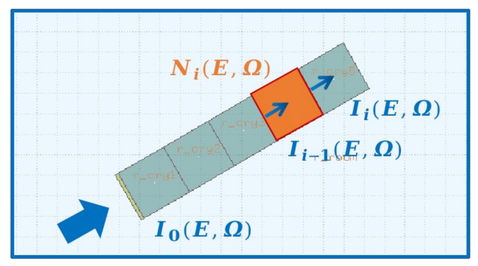

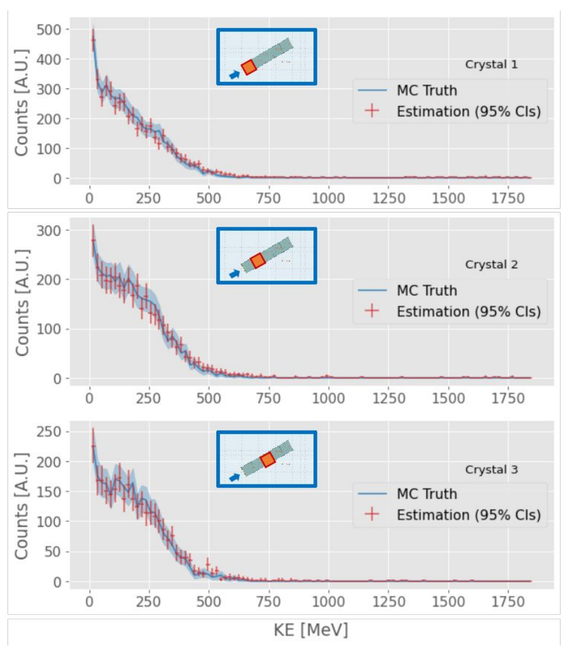

Figure 3 - Beer-Lambert fitting model (left). Neutron kinetic energy profiles at crystals 1-3 (right). Estimated values from TOF data (red). MC truth (blue). Shaded regions represent the 95% CIs.

Figure 4 shows the **estimated incoming neutrons** from the Beer-Lambert fit (red) and the MC truth values (blue) within the 95% confidence intervals for 20 MeV energy bins. The estimates follow the expected trend but exhibit a consistent offset, indicating underestimation. This is possibly due to neglecting neutron counts below detector sensitivity thresholds. This effect was modeled using a 1 MeV energy cutoff. Further investigation with a **detailed detector characterization at specialized neutron source installations** is required to estimate this offset.

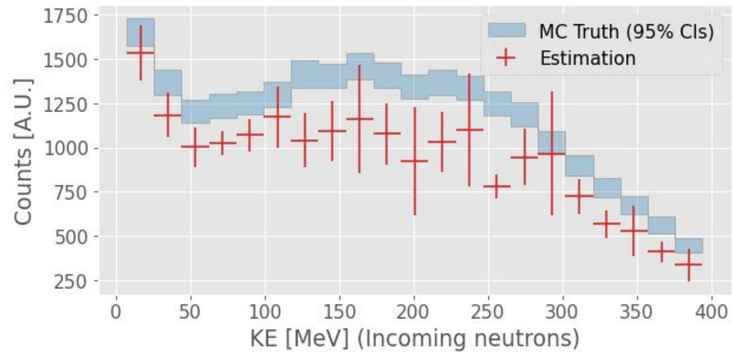

Figure 4 - Estimation of incoming neutrons per energy bin through Beer-Lambert fitting model. Estimated values (red) and 95% CIs MC truth of incoming neutrons (blue).

Conclusion

The proposed methodology substantially **shortens the experimental timescale** required for neutron measurements while maintaining accuracy and robustness under **high-rate operating conditions**. This performance relies on **photo-detectors capable of achieving sub-nanosecond time resolution** for precise TOF measurements. This accelerated acquisition may enable the generation of **extensive double-differential neutron production cross-sections** for diverse beam - target configurations, but also could be particularly suitable for applications in particle therapy and space radiation research, where efficient and reliable neutron characterization is essential.

References

[1] Vedelago J., et al., *Radiation Measurements*, 176, 107214, 2024, 10.1016/j.radmeas.2024.107214
[2] Norbury J.W., et al., *Frontier in Physics*, 8, 565954, 2020, 10.3389/fphy.2020.565954
[3] Krimmer J., et al., *Nuclear Instruments and Methods in Physics Research A*, 878, 2018, 10.1016/j.nima.2017.07.063